Graphdiyne Pores: 'Ad hoc' Openings for Helium Separation Applications

Massimiliano Bartolomei,[*,†] Estela Carmona-Novillo,[†] Marta I. Hernández,[†] José Campos-Martínez,[†] Fernando Pirani,[‡] and Giacomo Giorgi[¶]

Instituto de Física Fundamental, Consejo Superior de Investigaciones Científicas (IFF-CSIC), Serrano 123, 28006 Madrid, Spain, Dipartimento di Chimica, Biologia e Biotecnologie, Università di Perugia, Perugia, Italia, and Department of Chemical System Engineering, School of Engineering, University of Tokyo, Tokyo, Japan

E-mail: maxbart@iff.csic.es

[*]To whom correspondence should be addressed
[†]Instituto de Física Fundamental, Consejo Superior de Investigaciones Científicas (IFF-CSIC), Serrano 123, 28006 Madrid, Spain
[‡]Dipartimento di Chimica, Biologia e Biotecnologie, Università di Perugia, Perugia, Italia
[¶]Department of Chemical System Engineering, School of Engineering, University of Tokyo, Tokyo, Japan

Abstract

Two-dimensional (2D) materials deriving from graphene, such as graphdiyne and 2D polyphenylene honeycomb (2DPPH), have been recently synthesized and exhibit uniformly distributed sub-nanometer pores, a feature that can be exploited for gas filtration applications. Accurate first principles electronic structure calculations are reported showing that graphdiyne pores permit an almost unimpeded helium transport while it is much more difficult through the 2DPPH openings. Quantum dynamical simulations on reliable new force fields are performed in order to assess the graphdiyne capability for helium chemical and isotopic separation. Exceptionally high He/CH_4 selectivities are found in a wide range of temperatures which largely exceed the performance of the best membranes used to date for helium extraction from natural gas. Moreover, due to slight differences in the tunneling probabilities of ^{3}He and ^{4}He, we also find promising results for the separation of the fermionic isotope at low temperature.

KEYWORDS: graphynes, two-dimensional materials, nanofiltration, ab initio calculations

Introduction

Membranes using nanoporous two-dimensional (2D) materials are emerging as attractive candidates for applications in molecular separations and related areas.[1,2] In particular, graphene-based materials[3] exhibit vantage points with respect to conventional 3D materials, by virtue of their thermal and chemical stability as well as a low molecular weight and efficient transport capability. Graphene sheets do not have pores for molecular sieving and the introduction of sub-nanometer pores is required to obtain sufficient molecular permeance. This can be achieved by means of "top-down" fabrication methods able to create holes in suspended graphene sheets,[4] which, however, are in general not sufficiently controllable. "Bottom-up" assembly processes represent a valuable alternative and have permitted the synthesis of new 2D materials characterized by regular and uniformly distributed sub-nanometer pores. The most promising examples are graphdiyne[5] and 2D

polyphenylene honeycomb (2DPPH).[6] In the former, peculiar triangular pores arise from carbon chains formed by two conjugated C-C triple bonds that link adjacent benzene rings. In the latter, the resulting structure is instead similar to that of graphene but with one missing hexagon per unit cell which is passivated by hydrogens, leading to almost circular openings (see Fig. 1.a). The successful synthesis of these materials has led to important theoretical studies devoted, firstly, to their application as effective single-layer membranes for gas separation and water filtration technologies[7–11] and, secondly, to the tailoring of related porous 2D structures by changing pore shape and size through the incorporation of functional groups.[12–15]

In this work we want to assess the capability of the recently synthesized graphdiyne and 2DPPH materials as efficient membranes for helium separation applications. As it is well known, helium is an irreplaceable natural resource and its growing demand in a variety of industrial and scientific applications, together with ongoing production deficiencies, has recently led to shortages of this element.[16] Specifically, the lighter isotope, ^{3}He, is crucial for large neutron-scattering facilities and the depletion of its stockpiling might also affect fundamental research[17] in ultracold physics and chemistry. Natural gas remains the richest and most accessible source of helium even if its concentration is less than 1% in most of the helium-producing wells. Unfortunately most of the natural-gas plants treat helium as a valueless gas and vent it to the atmosphere. Therefore advanced and efficient technologies for its "in situ" recovery are highly desirable.

Existing methods for performing both the chemical separation of He from natural gas and the separation of He isotopes require energetically costly techniques, such as cryogenic distillation and pressure-swing adsorption.[18] In principle membrane-based gas separation has a much lower thermodynamic cost[19] and recent theoretical works have proposed the use of 2D membranes for the chemical[7,8,13,20] and isotopic[8,12,21,22] separation of He gas. In particular, studies on He permeability through 2DPPH membranes were already addressed[7,8] but, to our knowledge, the graphdiyne capability for He separation has not been investigated yet. Moreover, in our opinion, the reliability of the He–2DPPH penetration barriers, obtained by means of the density functional theory (DFT)[7] and second-order Møller-Plesset perturbation (MP2)[8] methodology, might need a deeper analysis.

The paper is organized as follows. Section 2 refers the computational methodologies for electronic structure calculations as well as the quantum mechanical tools used to calculate the penetration probabilities. In Section 3 we present our results concerning the barriers and the quantum simulations using new force fields, optimized from the electronic structure calculations. The paper ends with Section 4, in which some conclusions are summarized.

Computational Methods

The electronic structure calculations have been carried out at the "coupled" supermolecular second-order Møller-Plesset perturbation theory (MP2C)[23] level of theory by using the Molpro2012.1 package.[24] The geometry of the systems is that of Fig. 1.a, and for the pores we have considered the following bond lengths:[25] 1.431 Å for the aromatic C-C, 1.231 Å for triple C-C, 1.337 Å for the single C-C between two triple C-C bonds, 1.395 Å for the single C-C connecting aromatic and triple C-C bonds and 1.09 Å for C-H bonds. The aug-cc-pVTZ[26] basis set was employed for the pore structures, while the aug-cc-pV5Z[26] basis has been used for rare gases and methane molecule. All considered molecular structures are treated as rigid bodies: the atoms composing the investigated pores are frozen in their initial positions and the molecular configuration of methane is not allowed to relax during the calculations. The interaction energies have been further corrected for the basis set superposition error by the counterpoise method of Boys and Bernardi.[27]

For the calculation of the transmission probabilities of the atom/molecule through the pores we have employed a model that makes use of wave packet propagation. This technique is specially well suited for this system[28] since it is not necessary to invoke any periodicity and defects and many other interesting features can be naturally taken into account. The time-dependent Schrödinger equation was solved by propagating wave packets in a potential energy surface that is symmetric with respect to the origin, $V(-z) = V(z)$, where z represents the distance between the atom and the membrane. The initial wave packet is[29]

$$\psi(z,t=0) = \left(\frac{2Im(\alpha)}{\pi\hbar}\right)^{1/4} \times \exp\left\{\frac{i}{\hbar}\Big[\alpha(z-z_0)^2 + p(z-z_0)\Big]\right\}, \quad (1)$$

where $\alpha = 0.434\ i$ a.u., z_0 is a sufficiently large distance (typically 12-16 Å), and p is chosen such that $p^2/(2\mu)$ is close to the barrier height, where μ is the mass of the colliding particle. The wave packet is represented in a grid from $z = -L$ to $z = L$ (L= 50 Å) and is propagated using the split operator method.[30] The transmission probability is obtained by evaluating the probability current at the barrier ($z = 0$)[31,32]

$$P(E) = \frac{\hbar}{\mu} Im\left(\psi_E^{\star}(z=0)\frac{\partial\psi_E}{\partial z}|_{z=0}\right), \quad (2)$$

where ψ_E is the stationary wave function. It is computed from the Fourier transform of the time-dependent wave packet,

$$\psi_E(z) = \frac{1}{a(E)}\int dt\ e^{iEt/\hbar}\ \psi(z,t), \quad (3)$$

with

$$a(E) = C\int dz e^{ikz}\psi(z,t=0) \quad (4)$$

where $k = \sqrt{2\mu E}/\hbar$ and $C = \sqrt{\mu/(\hbar k)}$. It is important to note that, with this choice for the normalization of the stationary wave function, the probability current of Eq. (2) becomes adimensional and, in addition, it exactly corresponds to the transmission probability.[32,33]

Finally, the temperature-dependent transmission probability, $P(T)$, was computed from numerical integration of $P(E)$, weighted by a one-dimensional Maxwell-Boltzmann distribution of molecular velocities.

Results and Discussion

Penetration Barriers

In Fig. 1.a we report the molecular structures that can be considered as the smallest precursors[8,11] of graphdiyine and 2DPPH and which are here used to study their pores. It can be seen that, inside the pores, smaller black figures are also depicted. Their area corresponds to the effective pore size which has been estimated by considering the van der Waals (vdW) radii of the acetylenic carbon bonds, for graphdiyne, and of the inner hydrogen atoms, for 2DPPH ($\sim$ 1.6 Å and 1.3 Å, respectively). The side length of the inner triangle is 3.9 Å, for graphdiyne, and the diameter of the inner circle is 0.8 Å for 2DPPH. In the same way, the helium vdW diameter is 2.6 Å[34](represented by a double-headed arrow in Fig. 1.a) and it is smaller than the graphdiyne pore side but larger than the diameter of the 2DPPH circular opening. This comparison already suggests that He penetration should be easy in graphdiyne pores and more difficult when passing through the 2DPPH smaller pore.

A more quantitative assessment comes from electronic structure calculations. The prototypical systems of Fig. 1 are small enough to allow the use of the high level (and computationally expensive) MP2C approach and, at the same time, they are large enough to describe the interaction features of the pores, as demonstrated by test calculations in which we have considered further prototypes of increasing size. The accuracy of the MP2C method, which is particularly suited to recover non-covalent weak interactions, has been recently assessed by extensive calculations of rare gas–fullerene[35] and -coronene[36] interaction energies and it was concluded that the MP2C results are in good agreement with density functional theory-symmetry adapted perturbation theory (DFT-SAPT)[37] calculations, with the advantage of a significantly lower computational cost. In Fig. 1.b we report the calculated potential energy profiles for one helium atom perpendicularly approaching the 2D structures. In particular, z is the distance between helium and the geometric center of the pores. It can be seen that the penetration barrier (defined as the energy difference between z=0 and ∞, E_{PB}) is high (about 0.516 eV) for 2DPPH but becomes much lower (about

0.033 eV) for graphdiyne.

The He–2DPPH penetration barrier was previously obtained by means of MP2 and DFT calculations and found to be 0.523[8] and 0.430[7] eV, respectively. Our estimation is in between the previous calculations and closer to the MP2 value. Present value should be considered as the reference one since, to our knowledge, the employed dispersion corrected DFT approach[7] has not been sufficiently tested on this specific system. In fact we have determined that the calculated penetration barrier may vary depending on both the adopted density functional and 'a posteriori' empirical dispersion correction. Also, in our opinion the MP2 estimation[8] has been obtained by using basis sets (cc-pVDZ and cc-pVTZ) not sufficiently extended, thus neglecting diffuse functions that we have found to be important to properly describe the interaction in this system. Moreover the standard MP2 approach lacks the correction included in the MP2C method[23] which is indeed needed to improve the description of non-covalent interactions.[35] As an example, we have estimated that by using the same basis set the penetration barrier at the MP2 level of theory would be about 7% larger than present MP2C value. As for the He–graphdiyne system, it should be stressed that the calculated barrier of few tens of meV is not only much lower than that for 2DPPH, but also represents an energy gap comparable with other proposed 2D materials which, however, have not been fully synthesized yet. They include partially nitrogen functionalized porous graphene[12] (about 0.025 eV) and porous graphene-E-stilbene-1[13] (about 0.050 eV).

Barrier heights could be further reduced if the optimization of the position of the atoms defining the pores is taken into account. In fact, related additional calculations at the density functional level of theory (DFT) have been performed by considering the full "periodic" structure of a single graphdiyne layer and we have found that the barrier can lower by about 15% due to the deformation of the pores (see Fig. S1 of the Supporting Information).

To examine the efficiency of the two kinds of pores for helium permeation in more detail, we have considered a simple Arrhenius behavior for the diffusion rate D as a function of the temperature T: $D(T) = A_0 e^{\frac{-E_{PB}}{kT}}$, where E_{PB} is the computed penetration barrier. As it is custumary in this context[7,14,20] we have taken the same diffusion prefactor A_0=10^{11}s^{-1} for both pores. The

related diffusion rates are reported in Fig. 1.c and it can be seen that graphdiyne exhibits a much higher permeability than 2DPPH in an ample range of temperature, being the difference of about eight orders of magnitude at room temperature. These results clearly show that, due to its "ad hoc" pore size, a graphdiyne membrane is much more suited than the 2DPPH one for helium permeation and in the following we will focus on the former, analyzing in detail its separation capabilities.

In order to investigate the separation of helium from natural gas, we have considered neon and methane as limiting cases of the complex mixture of alkanes and rare gases therein usually present. Thus, additional accurate energy profiles are reported in Fig. 2 (upper panel) and compared with that of helium. It should be pointed out that methane is considered as a pseudo-atom, so that the reported energy profile is actually an average of different potential curves(see Supp. Inf. and Fig. S2). We find that this approximation is reasonable since the collision time t_c (the average time taken to cross the barrier) is about 2.5 times larger than the average CH_4 rotational period, t_r, for temperatures ranging from 100 to 300 K.[38,39] We have found that the penetration barrier E_{PB} (also reported in Table 1) for Ne and CH_4 increases up to 0.106 and 1.460 eV, respectively, suggesting a high impediment to the passage of methane.

Force Fields and Quantum Dynamical Simulations

To assess the separation capability of the graphdiyne pores, we have computed transmission probabilities for the passage of these species by means of time-dependent wave packet simulations. A new force field, optimized on the benchmark MP2C electronic structure results, has been obtained to this end. It provides the basic features of the interaction in the full configuration space, and therefore it is suitable for performing molecular dynamics simulations. Specifically, for describing the non-covalent interaction between the rare gas (and methane in the pseudo-atom limit) and the carbon atom forming the graphdiyne net structure the Improved Lennard-Jones (ILJ) pair potential function[40] is used:

$$V_{rg,c}(R) = \varepsilon \left[\frac{6}{n(x)-6} \left(\frac{1}{x}\right)^{n(x)} - \frac{n(x)}{n(x)-6} \left(\frac{1}{x}\right)^{6} \right] \quad (5)$$

where x is a reduced pair distance $x = \frac{R}{R_m}$, and ε and R_m represent the well depth and equilibrium distance of the rare gas(methane)-carbon interaction, respectively. Moreover, $n(x)$ is expressed by[41] $n(x) = \beta + 4.0\, x^2$ where β is a parameter defining the shape of the potential and depending on the nature and hardness of the interacting partners. The optimized ILJ parameters are reported in Table 1. They have a physical meaning, since they have been obtained by fine tuning initial data estimated by exploiting the polarizability values of the interacting partners. In the case of the graphdiyne pore, the average effective polarizability of the C atom has been used. In particular, a value equal to 1.1Å^3, consistent with that reported by Gavezzotti[42] describing the average behavior of C atom in various aliphatic and unsaturated molecules, has been adopted to estimate the dispersion energy contribution and the ε parameter associated to each rare gas (methane)-C interacting pair (see also Ref.[43]). Moreover, many-body effects have been also taken into account in the evaluation of the R_m values according to Ref.[44]

Additional MP2C energy curves for approaches of the atom (molecule) to different sites of the graphdiyne pore have been computed and taken into account (see Fig. 3) in order to more extensively test the features of the involved force field. In the upper panel of Fig. 2 (and in Fig. 3) we present a comparison between MP2C and ILJ curves and a very good agreement can be observed which confirms the reliability of the proposed force fields.

For simplicity we have just considered a one-dimensional transmission[8,12] of the atom through the center of a graphdiyne pore, where the interaction potentials have been obtained by summing up ILJ pair potentials between the atom (molecule) and the neighboring carbon atoms of a graphdiyne sheet until convergence. Values of the penetration barriers obtained in this way are reported in Table 1. Thermally weighted transmission probabilities $P(T)$ have been computed and used to estimate selectivities of the different molecular combinations X/Y, defined as the probability ratios $S = P^X/P^Y$. The temperature dependence of these selectivities is presented in the lower panel of Fig. 2. Exceptionally high selectivities can be noticed for He/CH_4 and Ne/CH_4 combinations in a

wide range of temperatures and they are about 10^{24} and 10^{23}, respectively, at room temperature. As for the He/Ne combination, the corresponding selectivity is about 27 at room temperature, suggesting a less efficient capability for the separation of these species, but in any case larger than 6, the value considered acceptable for industrial applications.[45] It should be noticed that the predicted selectivities could be actually reduced if the lowering of the penetration barrier due to deformation of the pores is taken into account: for the heavier species the larger lowering is expected (see Fig. S1) even if we do not consider that this effect can alter significantly the very favourable He/CH_4 and Ne/CH_4 probability ratios we have found. Further effects due to the neglect of both the interaction and competition of single components in the gas mixtures are not expected to provide significant deviations[13] in the obtained *S* behavior at least around and above room temperature.

Our results clearly indicate that the combination of a very high He diffusion rate (Fig. 1) and very high He/CH_4 and Ne/CH_4 selectivities (Fig. 2) makes graphdiyne a very promising material for the separation of He and Ne from the hydrocarbons contained in natural gas (higher alkanes, also present in natural gas, are expected to have even smaller transmission probabilities due to their larger size). As a matter of fact, due to the very low He and Ne concentrations in most of the natural gas reservoirs, very high selectivities (about 1000[46]) are required. This stringent requirement is indeed largely overcome by present estimations and, to our knowledge, not achieved by the polymeric membranes proposed up to date (corresponding selectivities are about 100[47]).

The high permeability that we have found for He-graphdiyne has encouraged us to study the possibility of separation of its isotopic variants. In particular, the separation of ^{3}He and ^{4}He could be achieved by taking advantage of slight differences in the tunneling probabilities of the two isotopes and by exploiting them in multistage processes,[22] which involve the passage of the gas through a number of graphdiyne layers. To this end we have computed transmission probabilities for ^{3}He and ^{4}He as functions of kinetic energy. The results are given in the upper panel of Fig. 4. It can be seen that, for kinetic energies lower than the classical barrier (see last column of Table 1), the ^{3}He transmission probability is significantly higher than that of ^{4}He, while the opposite occurs

for higher kinetic energies. For this reason, it makes sense to keep the gas temperature as low as possible in order to exploit the low energy side of the transmission curve.

Thermally weighted transmission probabilities as well as the corresponding ^{3}He/^{4}He selectivity as a function of temperature are reported in Fig. 4 (lower panel). It should be stressed that, for simplicity, we have assumed a (classical) Boltzmann distribution for kinetic energies of both isotopes instead of the intrinsic quantum statistics of fermionic ^{3}He and bosonic ^{4}He atoms. However, if a mixed nonideal quantum gas was considered, an even larger ^{3}He/^{4}He selectivity would be expected since the Fermi-Dirac distribution is broader than the Bose-Einstein one. Therefore, present estimation for the isotopic selectivity at 77 K (liquid nitrogen temperature) is about 1.04 and increases rapidly at low temperatures reaching the acceptable reference value of 6[45] at about 20 K. However, as the temperature drops, the transmission probabilities considerably decrease, as well as the He flux. In fact at 20K the ^{3}He transmission probability, even if larger than that of ^{4}He and of the classical limit (see lower panel of Fig. 4), is quite low and in the range of 10^{-9}.[48] The overall flux is the transmission probability multiplied by the frequency of gas collisions with the pore, which, according to the kinetic theory of gases, is $P/\sqrt{2\pi\mu kT}$ where P is the pressure of the species, T the temperature and k the Boltzmann constant. If we assume a 100% porous sheet, ideal gas conditions and a pressure of 3 bar we can estimate an upper-bound[49] of the total helium flux: at 77K it is about $3.7{\cdot}10^{-3}$ moles cm^{-2} s^{-1} while at 20K is about $1.5{\cdot}10^{-8}$ moles cm^{-2} s^{-1}, a value leading to a permeance[50] equal to $1.5{\cdot}10^{-8}$ moles cm^{-2} s^{-1} bar $^{-1}$ which is slightly lower than the limit of $6.7{\cdot}10^{-8}$ moles cm^{-2} s^{-1} bar $^{-1}$[45] considered acceptable for industrial applications.

Conclusions

In summary, by means of electronic structure MP2C computations, we have shown that graphdiyne is much more suited than 2DPPH for helium permeation since it involves a much lower penetration barrier (of the order of few tens of meV). Additional calculations of the interaction of neon and methane with a graphdiyne pore have allowed us to setup reliable full force fields which have

been used to compute quantum mechanical probabilities and selectivities for the passage of gases through the openings. We have found exceptionally favorable He/CH_4 and Ne/CH_4 selectivities in a wide range of temperatures which largely exceed the performance of the best membranes used for helium chemical separation. Thermally weighted helium tunneling calculations have been also performed to show selective transmissions of ^3He versus ^4He. For temperatures below 100K the $^3He/^4He$ selectivity becomes appreciably larger than 1, reaching an acceptable value of 6 at about 20K. We thus propose that, in addition to its promise for hydrogen[9] and water[11] purification, a graphdiyne based membrane can be efficiently used for helium separation applications addressed to filtering natural gas and, possibly, isotopic mixtures. On the basis of present results, since species other than helium are assumed to provide penetration barriers whose values increase with their vdW diameter, we consider that graphdiyne pores should also provide favorable selectivities for He/Ar, He/Kr and He/N_2 gas combinations which could permit optimal separation of helium from heavier rare gases and hydrothermal spring gases, the latter primarily composed of nitrogen.[51]

A full assessment of the capability of graphdiyne for helium isotopic separation would actually require three-dimensional simulations in order to better estimate the helium permeance at low temperatures and to take into account for zero-point energy effects due to in-pore vibrational modes. Work in this direction, by using the ILJ full force field, is in progress.

Acknowledgments

The work has been funded by Spanish grants FIS2010-22064-C02-02 and FIS2013-48275-C2-1-P. Allocation of computing time by CESGA (Spain) is also acknowledged. F.P. acknowledges financial support from the Italian Ministry of University and Research (MIUR) for PRIN 2010-2011, grant 2010 ERFKXL_002.

Supporting Information

Periodic DFT calculations as well as intermolecular potentials related to different configurations used for graphdiyne pore–methane computations are reported in additional figures. This information is available free of charge via the Internet at http://pubs.acs.org.

References

(1) Wun-gwi, K.; Sankar, N. Membranes from Nanoporous 1D and 2D Materials: A Review of Opportunities, Developments and Chellenges. *Chem. Eng. Sci.* **2013**, *104*, 908–924.

(2) Zhao, Y.; Xie, Y.; Liu, Z.; Wang, X.; Chai, Y.; Yan, F. Two-Dimensional Material Membranes: An Emerging Platform for Controllable Mass Transport Applications. *Small* **2014**, in press.

(3) Jiao, Y.; Du, A.; Hankel, M.; Smith, S. C. Modelling Carbon Membranes for Gas and Isotope Separation. *Phys. Chem. Chem. Phys.* **2013**, *15*, 4832–4843.

(4) Fischbein, M. D.; Drndic, M. Electron Beam Nanosculpting of Suspended Graphene Sheets. *Appl. Phys. Lett.* **2008**, *93*, 113107.

(5) Li, G.; Li, Y.; Liu, H.; Guo, Y.; Li, Y.; Zhu, D. Architecture of Graphdiyne Nanoscale Films. *Chem. Commun.* **2010**, *46*, 3256–3258.

(6) Bieri, M.; Treier, M.; Cai, J.; Aït-Mansour, K.; Ruffieux, P.; Gröning, O.; Gröning, P.; Kastler, M.; Rieger, R.; Feng, X.; et al. Porous Graphenes: Two-dimensional Polymer Synthesis with Atomic Precision. *Chem. Commun.* **2009**, *45*, 6919–6921.

(7) Blankenburg, S.; Bieri, M.; Fasel, R.; Müllen, K.; Pignedoli, C. A.; Passerone, D. Porous Graphene as Atmospheric Nanofilter. *Small* **2010**, *6*, 2266–2271.

(8) Schrier, J. Helium Separation Using Porous Graphene Membranes. *J. Phys. Chem. Lett.* **2010**, *1*, 2284–2287.

(9) Cranford, S. W.; Buehler, M. J. Selective Hydrogen Purification Through Graphdiyne Under Ambient Temperature and Pressure. *Nanoscale* **2012**, *4*, 4587–4593.

(10) Lin, S.; Buehler, M. J. Mechanics and Molecular Filtration Performance of Graphyne Nanoweb Membranes for Selective Water Purification. *Nanoscale* **2013**, *5*, 11801–11807.

(11) Bartolomei, M.; Carmona-Novillo, E.; Hernández, M. I.; Campos-Martínez, J.; Pirani, F.; Giorgi, G.; Yamashita, K. Penetration Barrier of Water through Graphynes' Pores: First-Principles Predictions and Force Field Optimization. *J. Phys. Chem. Lett.* **2014**, *5*, 751–755.

(12) Hauser, A. W.; Schwerdtfeger, P. Nanoporous Graphene Membranes for Efficient ^{3}He/^{4}He Separation. *J. Phys. Chem. Lett.* **2012**, *3*, 209–213.

(13) Brockway, A. M.; Schrier, J. Noble Gas Separation using PG-ESX (X=1,2,3) Nanoporous Two-Dimensional Polymers. *J. Phys. Chem. C* **2013**, *117*, 393–402.

(14) Lu, R.; Meng, Z.; Rao, D.; Wang, Y.; Shi, Q.; Zhang, Y.; Kan, E.; Xiao, C.; Deng, K. A Promising Monolayer Membrane for Oxygen Separation from Harmful Gases: Nitrogen-substituted Polyphenylene. *Nanoscale* **2014**, *6*, 9960–9964.

(15) Ambrosetti, A.; Silvestrelli, P. L. Gas Separation in Nanoporous Graphene from First Principle Calculations. *J. Phys. Chem. C* **2014**, *118*, 19172–19179.

(16) Nuttall, W. J.; Clarke, R. H.; Glowacki, B. A. Resources: Stop Squandering Helium. *Nature* **2012**, *485*, 573–575.

(17) Halperin, W. P. The Impact of Helium Shortages on Basic Research. *Nature Physics* **2014**, *10*, 467–470.

(18) Das, N. K.; Chaudhuri, H.; Bhandari, R.; Ghose, D.; Sen, P.; Sinha, B. Purification of Helium from Natural Gas by Pressure Swing Adsorption. *Curr. Sci.* **2008**, *95*, 1684–1687.

(19) Bernardo, P.; Drioli, E.; Golemme, G. Membrane Gas Separation: A Review/State of the Art. *Ind. Eng. Chem. Res.* **2009**, *48*, 4638–4663.

(20) Hu, W.; Wu, X.; Li, Z.; Yang, J. Helium Separation Via Porous Silicene Based Ultimate Membrane. *Nanoscale* **2013**, *5*, 9062–9066.

(21) Hauser, A. W.; Schrier, J.; Schwerdtfeger, P. Helium Tunneling through Nitrogen-Functionalized Graphene Pores: Pressure- and Temperature-Driven Approaches to Isotope Separation. *J. Phys. Chem. C* **2012**, *116*, 10819–10827.

(22) Mandrà, S.; Schrier, J.; Ceotto, M. Helium Isotope Enrichment by Resonant Tunneling through Nanoporous Graphene Bilayers. *J. Phys. Chem. A* **2014**, *118*, 6457–6465.

(23) Pitonák, M.; Hesselmann, A. Accurate Intermolecular Interaction Energies from a Combination of MP2 and TDDFT Response Theory. *J. Chem. Theory Comput.* **2010**, *6*, 168–178.

(24) Werner, H.-J. et al. MOLPRO, Version2012.1, a Package of Ab Initio Programs. 2012; see-http://www.molpro.net.

(25) Pei, Y. Mechanical Properties of Graphdiyne Sheet. *Physica B* **2012**, *407*, 4436–4439.

(26) Kendall, R. A.; Dunning, T. H.; Harrison, R. J. Electron Affinities of the First-Row Atoms Revisited. Systematic Basis Sets and Wave Functions. *J. Chem. Phys.* **1992**, *96*, 6796–6806.

(27) Boys, S.; Bernardi, F. The Calculation of Small Molecular Interactions by the Differences of Separate Total Energies. Some Procedures with Reduced Errors. *Mol. Phys.* **1970**, *19*, 553–566.

(28) Hernández, M. I.; Campos-Martínez, J.; Miret-Artés, S.; Coalson, R. D. Lifetimes of Selective-Adsorption Resonances in Atom-Surface Elastic Scattering. *Phys. Rev. B* **1994**, *49*, 8300–8309.

(29) Heller, E. J. Time-Dependent Approach to Semiclassical Dynamics. *J. Chem. Phys.* **1975**, *62*, 1544–1555.

(30) Feit, M. D.; Jr., J. A. F.; Steiger, A. Solution of the Schrödinger equation by a spectral method. *J. Comput. Phys.* **1982**, *47*, 412–433.

(31) di Domenico, D.; Hernández, M. I.; Campos-Martínez, J. A Time-Dependent Wave Packet Approach for Reaction and Dissociation in H_2+H_2. *Chem. Phys. Lett.* **2001**, *342*, 177–184.

(32) Zhang, D.; Zhang, J. Z. H. Full-Dimensional Time-Dependent Treatment for Diatom-Diatom Reactions: The H_2+OH Reaction. *J. Chem. Phys.* **1991**, *101*, 1146–1156.

(33) Miller, W. H. Quantum Mechanical Transition State Theory and A New Semiclassical Model for Reaction Rate Constants. *J. Chem. Phys.* **1974**, *61*, 1823.

(34) Tang, K. T.; Toennies, J. P.; Yiu, C. L. Accurate Analytical He-He van der Waals Potential Based on Perturbation Theory. *Phys. Rev. Lett.* **1995**, *74*, 1546–1549.

(35) Hesselmann, A.; Korona, T. On the Accuracy of DFT-SAPT, MP2, SCS-MP2, MP2C, and DFT+DISP Methods for the Interaction Energies of Endohedral Complexes of the C(60) Fullerene with a Rare Gas Atom. *Phys. Chem. Chem. Phys.* **2011**, *13*, 732–743.

(36) Bartolomei, M.; Carmona-Novillo, E.; Hernández, M. I.; Campos-Martínez, J.; Pirani, F. Global Potentials for the Interaction Between Rare Gases and Graphene-Based Surfaces: An Atom-Bond Pairwise Additive Representation. *J. Phys. Chem. C* **2013**, *117*, 10512–10522.

(37) Hesselmann, A.; Jansen, G.; Schütz, M. Density-Functional Theory-Symmetry-Adapted Intermolecular Perturbation Theory with Density Fitting: A New Efficient Method to Study Intermolecular Interaction Energies. *J. Chem. Phys.* **2005**, *122*, 014103.

(38) Levine, R. D.; Berstein, R. B. *Molecular Reaction Dynamics and Chemical Reactivity*; Oxford University Press, New York, 1987.

(39) The collision time was estimated as $t_c = L/\langle v \rangle$, L being the range of the interaction (specifically, the distance from the van der Waals minimum to the barrier), and $\langle v \rangle$, the mean speed at a given temperature. Methane rotational time was computed as $t_r = 3\pi\hbar/[B\sqrt{J^\star(J^\star+1)}]$, where B is the rotational constant, $J^\star$ is the most probable angular momentum at a given temperature, and the factor three accounts for the symmetry of the molecule.

(40) Pirani, F.; Brizi, S.; Roncaratti, L.; Casavecchia, P.; Cappelletti, D.; Vecchiocattivi, F. Beyond the Lennard-Jones Model: A Simple and Accurate Potential Function Probed by High Resolution Scattering Data Useful for Molecular Dynamics Simulations. *Phys. Chem. Chem. Phys* **2008**, *10*, 5489–5503.

(41) Pirani, F.; Albertí, M.; Castro, A.; Teixidor, M. M.; Cappelletti, D. Atom-Bond Pairwise Additive Representation for Intermolecular Potential Energy Surfaces. *Chem. Phys. Lett.* **2004**, *394*, 37–44.

(42) Gavezzotti, A. Calculation of Intermolecular Interaction Energies by Direct Numerical Integration over Electron Densities. 2. An Improved Polarization Model and the Evaluation of Dispersion and Repulsion Energies. *J. Phys. Chem. B* **2003**, *107*, 2344–2353.

(43) Albertí, M.; Aguilar, A.; Lucas, J. M.; Pirani, F. Competitive Role of CH_4-CH_4 and CH-π Interactions in the C_6H_6-(CH_4)n Aggregates: The Transition from Dimers to Cluster Features. *J. Phys. Chem. A* **2012**, *116*, 5480–5490.

(44) Pirani, F.; Cappelletti, D.; Liuti, G. Range, Strength and Anisotropy of Intermolecular Forces in Atom-Molecule Systems: An Atom-Bond Pairwise Additivity Approach. *Chem. Phys. Lett.* **2001**, *350*, 286–296.

(45) Zhou, Z. Permeance Should Be Used to Characterize the Productivity of a Polymeric Gas Separation Membrane. *J. Membr. Sci.* **2006**, *281*, 754–756.

(46) Zolandz, R. R.; Fleming, G. In *Membrane Handbook*; Ho, W. S. W., Sirkar, K. K., Eds.; Kluwer Academic Publishers: Dordrecht, The Netherlands, 2001; pp 78–94.

(47) Díez, B.; Cuadrado, P.; Marcos-Fernández, A.; Prádanos, P.; A, T.; Palacio, L.; Lozano, A. E.; Hernández, A. Helium Recovery by Membrane Gas Separation Using Poly(*o*-acyloxyamide)s. *Ind. Eng. Chem. Res.* **2014**, *53*, 12809–12818.

(48) It should be noticed that, due to the pore relaxation, the reduction of the He penetration barrier can also lead to a higher ^{3}He trasmission probability which at 20K would be about $2{\cdot}10^{-8}$. The corresponding permeance would also increase to $2.4{\cdot}10^{-7}$ moles cm^{-2} s^{-1} bar $^{-1}$ leading to a better agreement with the acceptable value for industrial applications.

(49) We assume that any particle reaching the surface will always encounter a pore and that it will experience a potential energy barrier equals to that normal to the plane of the pore. In a more realistic simulation the helium flux is expected to be lower.

(50) Permeance (Q) is defined as the ratio between the flux and pressure drop across the pore, $Q = Flux/\Delta P$. In the present case we are assuming ΔP= 1 bar.

(51) Das, N. K.; Barat, P.; Sen, P.; Sinha, B. Enrichment of Helium from Hydrothermal gases. *Curr. Sci. India* **2003**, *84*, 1519–1524.

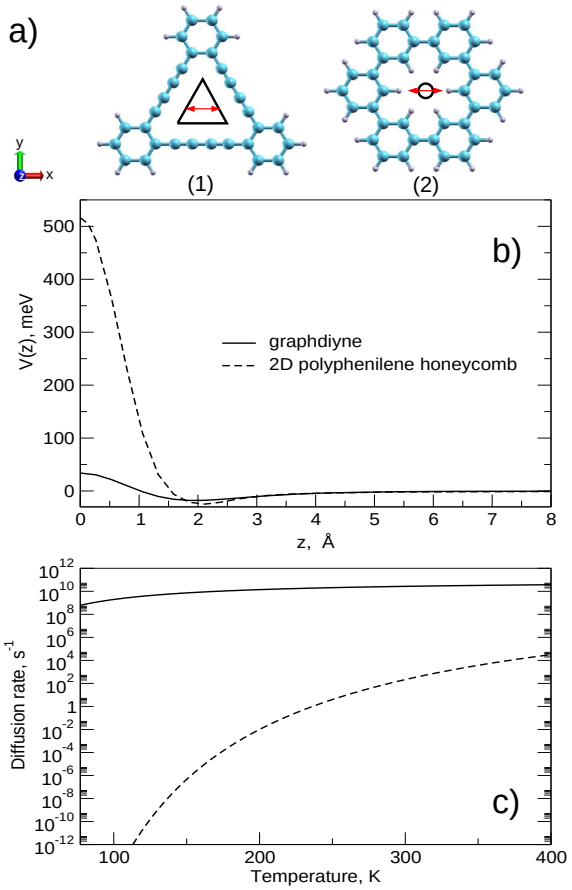

Figure 1: a) Molecular structures used to study the nano-pores of graphdiyne(1) and 2D polyphenylene honeycomb (2). The black triangle and circle depicted inside the pores represent their effective available area to be compared with the van der Waals diameter of the He atom (red double-headed arrow). b) Energy profiles obtained at the MP2C level of theory for He perpendicularly approaching the geometric center of graphdiyne and 2DPPH pores. c) Rates for He diffusion through the pores as functions of temperature (see text).

Table 1: Penetration barrier(E_{PB}) for He, Ne and CH_4 passage through graphdiyne pores. Parameters for the rare gas (methane)-carbon Improved Lennard Jones (ILJ) pair potential (see Eq. 5), used to obtain the full force fields, are also reported, together with the resulting penetration barriers after a pair-wise summation over a graphdiyne sheet. E_{PB} and ε are in meV, R_m in Å , and β is dimensionless.

		ILJ force field			
	$E_{PB}(MP2C)$	R_m	ε	β	$E_{PB}(ILJ)$
He	33.90	3.595	1.209	7.5	36.92
Ne	105.76	3.671	2.388	7.5	109.17
CH_4	1460.31	4.046	7.763	7.5	1454.70

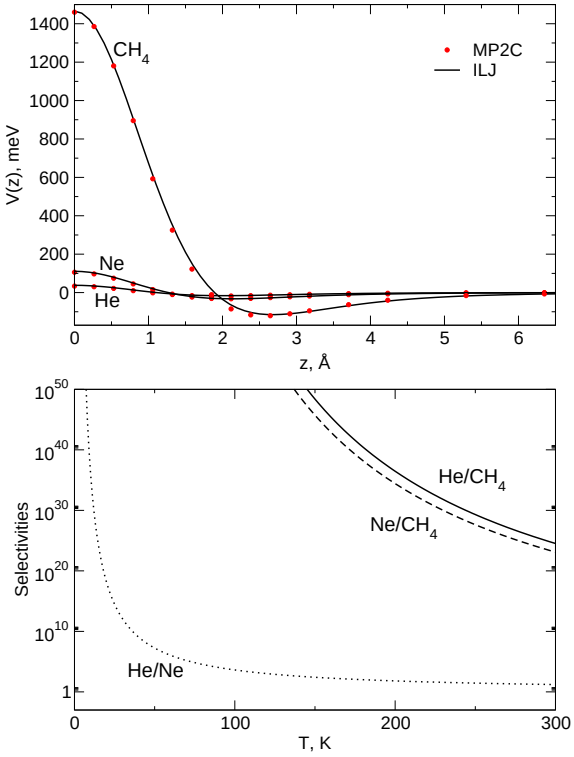

Figure 2: Upper panel: Energy profiles obtained for helium, neon and methane perpendicularly approaching the geometric center of the graphdiyne pore. In the case of methane the resulting curve is the average of four limiting configurations (see Fig. S2). Red dots refer to the MP2C level of theory results while solid curves represent estimations obtained with optimized Improved Lennard Jones (ILJ) force fields (see text). Lower panel: Selectivities for different molecular combinations as functions of temperature(see text).

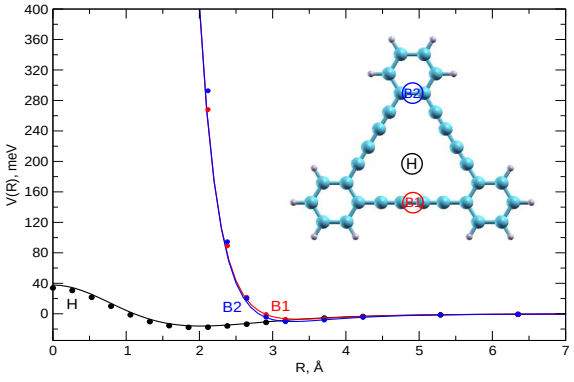

Figure 3: Interaction profiles for the approach of the helium atom to three different sites (H, B1 and B2) of the graphdiyne pore. Circles correspond to the MP2C *ab initio* results while solid lines represent ILJ full force field predictions.

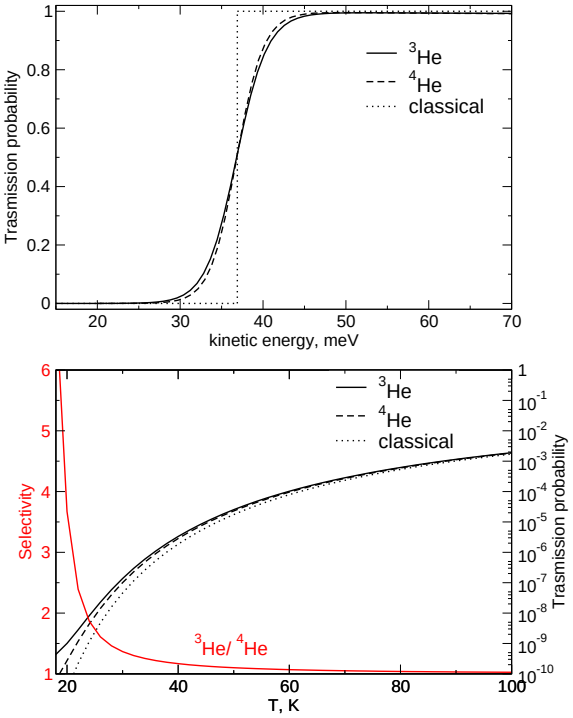

Figure 4: Upper panel: Quantum mechanical and classical transmission probabilities of He through graphdiyne pore as a function of kinetic energy. Lower panel: ^{3}He/^{4}He selectivity (red line) and thermally weighted quantum transmission probabilities (solid and dashed black lines for ^{3}He and ^{4}He, respectively) as functions of temperatures. Classical transmission probability is reported as a dotted line.

Table of Content

Graphdiyne is a novel two-dimensional material deriving from graphene that has been recently synthesized and featuring uniformly distributed sub-nanometer pores. Accurate calculations are reported showing that graphdiyne pores permit an almost unimpeded helium transport which can be employed for its chemical and isotopic separation. Exceptionally high He/CH_4 selectivities are found which largely exceed the performance of the best membranes used to date for extraction from natural gas. Moreover, by exploiting slight differences in the tunneling probabilities of ^{3}He and ^{4}He, we also find promising results for the separation of the fermionic isotope at low temperature.